AIAA 80-0723R

Multilevel Optimum Design of Structures with Fiber-Composite Stiffened-Panel Components

Lucien A. Schmit* and Massood Mehrinfar†
University of California, Los Angeles, Calif.

The multilevel approach to minimum weight structural design is extended to wing box structures with fiber-composite stiffened-panel components. Strength, deflection, and panel buckling constraints are treated at the system level with equivalent-thickness-type design variables. Local buckling and panel buckling constraints are guarded against at the component level, employing detailed component dimensions as design variables. A key feature of the method is selection of change in stiffness as the component level objective function to be minimized. Numerical results are given for wing box structures with sandwich and hat-stiffened fiber-composite panels.

I. Introduction

In this paper, the multilevel approach to minimum weight structural design is extended to wing box structures with fiber-composite stiffened-panel components. Minimum weight designs are sought while guarding against a variety of failure modes, including panel and/or local buckling as well as excessive strain levels and displacements.

In the context of minimum weight design of structural systems involving local buckling constraints, Refs. 1 and 2 present a simplified direct method for minimum weight design of tubular truss structures. Adopting the simultaneous failure mode approach, an intuitive knowledge of the critical failure modes which characterize the optimum design is used to reduce the dimensionality of the design problem by a factor of two. The tubular truss synthesis problem is formulated in terms of area variables and the detailed design variables (diameters and thicknesses) are calculated at the end of structural synthesis using the known areas and the diameter/thickness ratios corresponding to the optimum stress values. A serious disadvantage of the direct approach set forth in Refs. 1 and 2 is the omission of side constraints, which frequently leads to component designs with impractically large diameter/thickness ratios. In a recent work[3] this method is extended to include side constraints on the diameter and thickness of thin-walled tubular truss components. The approach employed in Refs. 1-3 avoids the multilevel approach by finding closed-form solutions for the component level synthesis problems. However, for structural systems involving more complex components, such as fiber-composite stiffened panels, the multilevel approach continues to be attractive, because each component level design task often involves several detailed design variables and relatively complex buckling failure mode analyses.

Early applications of the multilevel approach to minimum weight design of wing and fuselage structures were reported in Refs. 4 and 5, respectively. While the basic multilevel idea set forth in Refs. 4 and 5 is sound, the implementation suffered from two main shortcomings, namely, 1) the use of weight as the objective function at the component level and 2) the use of fully stressed type resizing algorithms at the system level. As recognized in Ref. 5, the minimum weight structural system is not necessarily made up from a collection of minimum weight components. To cope with this problem, Ref. 6 introduced a multilevel approach wherein the system and component level design phases are characterized as follows: 1) reduce the total structural weight subject to the system level constraints such as displacement, system buckling, strength, etc., and 2) minimize the change in each components equivalent system stiffness, subject to local and panel buckling constraints. The system level design improvement scheme employed here is based on the work reported in Ref. 7, where approximation concepts (such as design variable linking, temporary deletion of inactive constraints, and high quality explicit approximations for retained constraints) are used to achieve efficiency. In Ref. 6 the multilevel approach was applied to the minimum weight design of wing box structures with integrally stiffened waffle plate components. Here the multilevel method is improved and extended to wing box structures with sandwich and hat-stiffened fiber-composite panels.

II. Formulation

The inclusion of local buckling constraints in addition to the usual stress, displacement, and member size limitations treated in Refs. 7-9 presents difficulties because their meaningful representation requires that some consideration be given to the detail design of the many individual components which make up the structural system. Inclusion of all of the detailed variables of the components in a single large mathematical programming problem statement rapidly increases the number of design variables, and a direct attack on the problem in this form is impractical.

The multilevel concept appears to be a sound basic approach for minimum weight design of large structural problems involving local buckling constraints that are strongly dependent on detailed design variables, as well as displacement and strength constraints that are functions of system design variables (smeared-stiffener equivalent-thickness representation of the components). The general multilevel approach is described schematically in Fig. 1. The formulation employed here represents a heuristic decomposition, guided by physical insight, which breaks the primary problem statement into a system level design problem and a set of uncoupled component level problems. Results are obtained by iterating between the system and component level problems.

Let $\boldsymbol{D}$ represent the set of system design variables and $\boldsymbol{d}_j$ represent the set of component design variables for the jth component. Then the problem can be stated as follows: Find

Presented as Paper 80-0723 at the AIAA/ASME/ASCE/AHS 21st Structures, Structural Dynamics and Materials Conference, Seattle, Wash., May 12-14, 1980; submitted July 2, 1980; revision received June 15, 1981.

*Professor of Engineering and Applied Science, Mechanics and Structures Dept., School of Engineering and Applied Science. Associate Fellow AIAA.

†Postdoctoral Research Associate, Mechanics and Structures Dept., School of Engineering and Applied Science. Member AIAA.

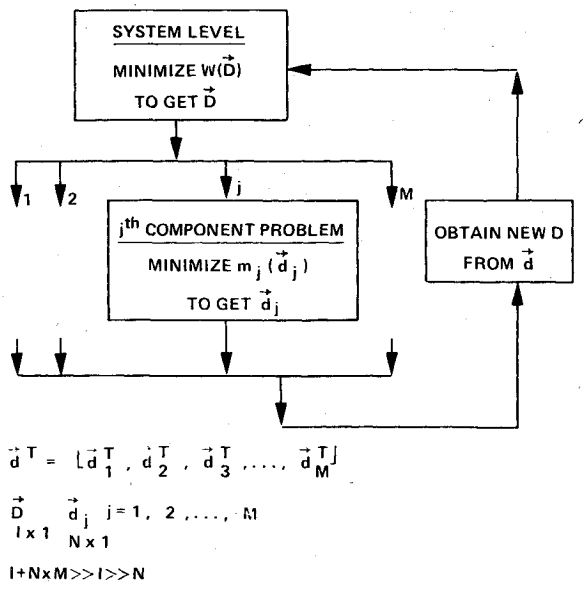

Fig. 1 Multilevel approach.

D and $d_1, d_2, d_3, \ldots, d_M$

$$W(D) \rightarrow \min \tag{1}$$

and

$$G_q(D,d) \geq 0 \qquad q \in Q \tag{2}$$

and

$$g_{ij}(d_j,D) \geq 0 \qquad \ell \in L \quad j \in M \tag{3}$$

$G_q(D,d)$ represent constraints that are strongly dependent on the vector of system design variables D and are implicit functions except for the side constraints. $g_{ij}(d_j,D)$ represent constraints that are primarily dependent on the design variables d_j describing the jth component in detail, and are either explicit or implicit functions of d_j, depending on the kind of constraints and the type of local buckling analysis used. The symbols Q and L denote the set of system and component level constraints, respectively, M denotes the number of components, and $d^T = [d_1^T, d_2^T, d_3^T, \ldots, d_M^T]$.

The multilevel approach presented in Ref. 6 suggests that the structural synthesis problem given by Eqs. (1-3) be reorganized into two levels of design modification as follows:

System level: Find D such that

$$W(D) \rightarrow \min \tag{4}$$

and

$$\tilde{G}_q(D,d^*) \geq 0 \qquad q \in Q_R \tag{5}$$

where d^* indicates invariance of the detailed design variables and implies that parameters such as the allowable buckling loads do not change during a system level design modification stage, $\tilde{G}_q$ indicates the use of explicit approximations (see Refs. 7 and 8) for the system level constraints, and Q_R represents the reduced set of system level constraints retained after deletion of those that are neither critical nor potentially critical.

Component level for each component ($j=1,2,\ldots,M$): Find d_j such that

$$m_j(d_j) \rightarrow \min \tag{6}$$

and

$$g_{ij}(d_j,D^*) \geq 0 \qquad \ell \in L \tag{7}$$

where D^* indicates invariance of the system level design variables and implies that parameters such as panel strains are held constant during each component design modification stage. The component objective function $m_j(d_j)$ is chosen so as to minimize the change in component stiffness. In general the stiffness characteristics of the jth component depend on a set of R stiffness parameters which can be expressed as explicit functions of the system design variables or the component design variables. Therefore the jth component objective function is given by

$$m_j = \sum_{r=1}^{R} [K_{rj}(D_j^*) - H_{rj}(d_j)]^2 \tag{8}$$

where $K_{rj}(D_j^*)$ is the rth stiffness characteristic of the jth component in terms of the corresponding system design variables obtained at the end of a system design modification. These values are held invariant during the component design modification. The symbol $H_{rj}(d_j)$ represents the rth stiffness characteristic of the jth component expressed as an explicit function of detailed design variables. The detailed design variables obtained at the end of the sth component design modification stage $d_j^{(s)}$ are used to calculate the initial design $D_j^{(s+1)}$ for the $(s+1)$th system design stage. Note that system level equivalent thicknesses can be expressed explicitly in terms of detailed design variables. If at any stage s, the component design objective function m_j becomes zero, then each $H_{rj}(d_j^{(s)})$ will be equal to the corresponding $K_{rj}(D_j^{(s)})$. If m_j goes to zero for all $j=1,\ldots,M$, then there is no force redistribution at the system level as a result of the detailed component design modification.

Selecting change of stiffness as the component level objective function to be minimized and using relatively tight move limits at the system level weakens the coupling between the two levels of design modification, thus enhancing convergence of the overall design procedure.

III. Optimization Procedure

The optimization procedure employed for both system and component synthesis is based on the quadratic extended interior penalty function set forth in Ref. 10. This formulation leads to a sequence of unconstrained minimization problems, each of which is solved using the modified Newton method presented in Ref. 11. The use of this algorithm, which is called NEWSUMT (see Refs. 7-9), plays a central role in the multilevel approach as implemented here, since it tends to produce a sequence of noncritical designs that "funnel down the middle" of the feasible region. The NEWSUMT algorithm is also well suited to coping with the highly nonlinear buckling constraints involved in the component optimization problems.

A component design modification stage consists of a complete component synthesis for each independent component. Normally, in treating the component optimization problems constraint deletion and Taylor series expansions are not employed because: 1) the panel and local buckling constraints can be expressed explicitly in terms of the component design variables using conventional buckling analysis simplifications, 2) each independent component optimization problem involves a relatively small number of design variables and constraints. However, if it became necessary to employ more complex component level buckling analyses, involving the solution of eigenproblems, then the use of constraint deletion and Taylor series expansions to generate explicit constraint approximations would be appropriate.

At the system level all of the approximation concepts introduced in Refs. 7-9 are employed. Expressing the system design problem given by Eqs. (4) and (5) in terms of linked reciprocal variables α and using the quadratic extended interior penalty function, the problem statement is transformed into a sequence of unconstrained minimizations of the form

$$\phi_e(\alpha, r_a) = W(\alpha) + r_a \sum_{q \in Q_R} \tilde{F}_q(\alpha) \tag{9}$$

where

$$\tilde{F}_q(\alpha) = 1/\tilde{G}_q(\alpha) \qquad \text{if } \tilde{G}_q \geq \epsilon$$

$$= \frac{1}{\epsilon}\left[\frac{1}{\epsilon^2}\tilde{G}_q^2 - \frac{3}{\epsilon}\tilde{G}_q + 3\right] \text{ if } \tilde{G}_q < \epsilon \tag{10}$$

and ϕ_e is minimized with respect to α for a decreasing sequence of values

$$r_{a+1} = c_a r_a \qquad 0 < c_a < 1 \tag{11}$$

The $F_q(\alpha)$ defined by Eq. (10) is continuous and it has continuous first and second derivatives at the transition point defined by $\tilde{G}_q(\alpha) = \epsilon$. The unconstrained minimization of $\phi_e(\alpha, r_a)$ is accomplished by executing a series of one-dimensional minimizations along directions established by the modified Newton Method.

The use of the interior penalty function formulation in conjunction with relatively tight move limits at the system level tends to generate a sequence of gradually changing designs that are not critical with respect to behavioral constraints. At the component level the constraint repulsion characteristics inherent to the interior penalty function formulation tend to generate component design modifications with improved panel buckling allowables. Thus the use of the interior penalty function formulation at both levels helps to minimize coupling between the system and component optimization problems.

IV. Structures with Fiber-Composite Panel Components

The feasibility of extending the multilevel approach to fiber composite panels is initially established by focusing attention on wing box structures with sandwich-panel components. Hat-stiffened fiber-composite panels are considered subsequently. For sandwich panels with laminated fiber-composite face sheets (see Fig. 2) the component level design variables are the core depth (C), the orthotropic core shear areas A_{xz} and A_{yz}, and the thicknesses of fiber-composite material oriented at 0° (t_1), ±45° (t_2), and 90° (t_3) in the symmetric face sheets. To simplify the sandwich-panel feasibility study the shear core areas A_{xz} and A_{yz} are treated as fixed parameters and the sandwich plate buckling analysis neglects shear core deformation. Therefore each sandwich panel is described by four independent component level design variables (namely, C, t_1, t_2, t_3). At the system level each fiber-composite sandwich panel is modeled by stacking four orthotropic assumed stress rectangular plate elements representing equivalent thicknesses of material oriented in the 0° ($t^{(1)}$), +45° ($t^{(2)}$), −45° ($t^{(3)}$), and 90° ($t^{(4)}$) directions (see Fig. 2). These assumed stress elements are called orthotropic linear stress rectangular (OLSR) elements and they allow for linear variation of σ_x in the y direction, linear variation of σ_y in the x direction, and constant τ_{xy}. They are well matched to the panel buckling analyses used at both the system and component levels and their use here constitutes an improvement over the relatively crude constant strain triangle (CST) elements employed in Ref. 6. The equivalent thicknesses of material in the +45° and the −45° directions are linked (i.e., $t^{(2)} = t^{(3)}$) in order to preserve the inplane orthotropy of the sandwich-panel face sheets. Therefore for each fiber composite sandwich panel there are three independent system level design variables.

On the other hand, for each fiber-composite hat-stiffened panel component three independent thicknesses (t_i) and four independent widths (b_i) are treated as design variables. Figure 3 shows the detailed design variables for a fiber-composite hat-stiffened panel of the type studied extensively in Refs. 12 and 13. The thickness of ±45° material in the cap (element 3) and sides (element 2) of the hat stiffener is the same as the thickness of ±45° material in the backup sheet above the stiffener (element 1), therefore $t_1(\pm 45°) = t_2(\pm 45°)$. Furthermore, the thickness of ±45° material between the stiffeners (element 4) is twice that of the ±45° material in the sides and cap of the hat stiffener. The thicknesses of the two equal 0° layers in element 3 are denoted by $t_3(0°)$. Furthermore, $t_4(0°)$ represents the thickness of a 0° layer sandwiched between ±45° skins in element 4. The quantities b_1, b_2, and b_3 are the widths of elements 1, 2, and 3, respectively. The quantity b_4 represents the half-width of element 4.

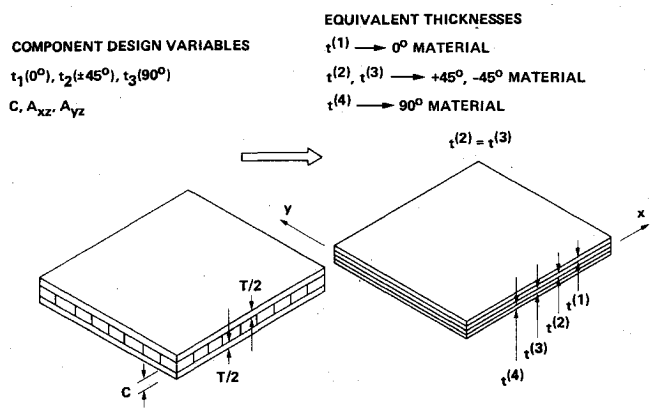

Fig. 2 System idealization of fiber-composite sandwich component.

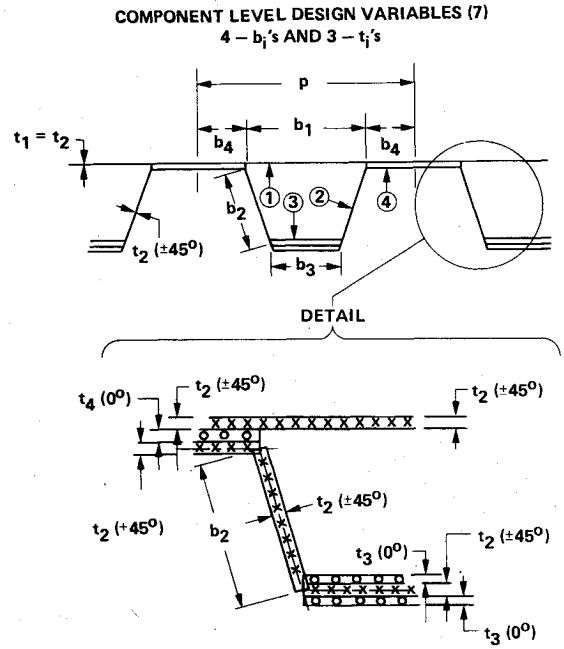

Fig. 3 Fiber-composite hat-stiffened component.

At the system level, each fiber-composite hat-stiffened panel is idealized by stacking five orthotropic assumed stress rectangular plate elements representing equivalent thicknesses of 0° material ($t^{(1)}$), +45° ($t^{(2)}$), and −45° ($t^{(3)}$) material in the backup sheet, and +45° ($t^{(4)}$) and −45° ($t^{(5)}$) material in the stiffener (see Fig. 4). Since the 0° material carries only axial force in the direction of the stiffeners, the modulus of elasticity in this direction is the only nonzero stiffness property for the corresponding OLSR element. Also, the finite elements representing the +45° and −45° material in the stiffeners will be taken to have zero modulus of elasticity transverse to the hat stiffeners. The equivalent thicknesses of material at +45° and −45° are linked to preserve orthotropy

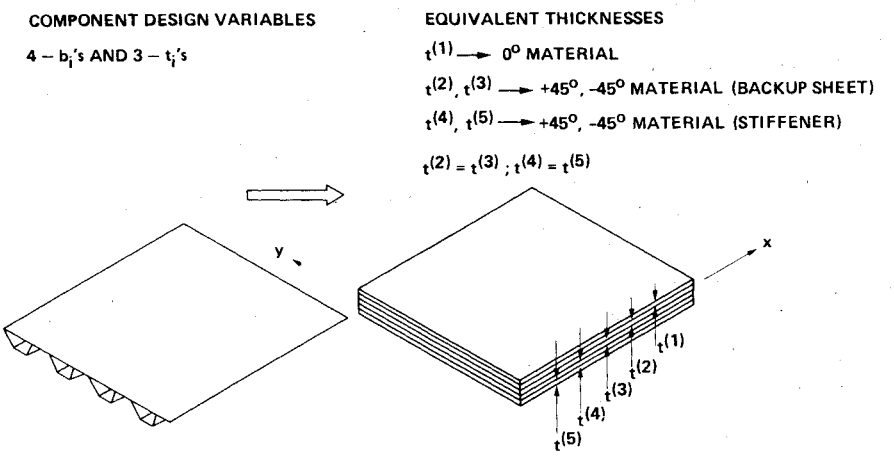

Fig. 4 System idealization of fiber-composite hat-stiffened component.

of the panel (i.e., $t^{(2)} = t^{(3)}$ and $t^{(4)} = t^{(5)}$). As a result, there are three independent system level design variables per hat-stiffened panel and they can be expressed in terms of the component level design variables as follows:

$$t^{(1)} = (2t_2b_3 + 2t_4b_4)/(b_1 + 2b_4) \tag{12}$$

$$t^{(2)} = t^{(3)} = t_2/2 \tag{13}$$

$$t^{(4)} = t^{(5)} = \frac{t_2b_2 + (t_2b_3/2) + t_2b_4}{b_1 + 2b_4} \tag{14}$$

Here, for the sake of simplicity, only midplane-symmetric wing-box structures are considered. Spar and rib caps (if any) are modeled using TRUSS elements, while webs are represented by symmetric shear panel (SSP) elements (see Ref. 8). The wing cover plates, comprised of fiber composite panel components, are idealized at the system level by merging a stack of OLSR elements. Therefore the system design variables ($\boldsymbol{D}$) include the cross-sectional areas (A_i) of TRUSS elements, thicknesses (τ_i) of SSP elements, and the thicknesses (t_i) of OLSR elements. Since most of the structural weight of wing box structures resides in the skin panels, detailed design considerations will be limited to these panels in this investigation.

System Level

The system level design optimization procedure is based on modification of the ACCESS 1 program (see Refs. 7 and 8) to include OLSR elements and panel buckling constraints of the form

$$1 - \left[\frac{N_x}{(N_x)_{cr}} + \frac{N_y}{(N_y)_{cr}} + \left(\frac{N_{xy}}{(N_{xy})_{cr}}\right)^2\right] \geq 0 \tag{15}$$

These panel buckling constraints are, strictly speaking, functions of both system and component level design variables. This is true because the system level force distribution, which yields the N_x, N_y, and N_{xy} terms, depends upon the system level design variables and the terms $(N_x)_{cr}$, $(N_y)_{cr}$, and $(N_{xy})_{cr}$ depend upon the detailed design variables describing the panel at the component level. Therefore in the multilevel approach approximate panel buckling constraints are introduced at both the system and the component level. At the system level the N_x, N_y, and N_{xy} are expressed as explicit functions of the system level design variables using Taylor series expansions in terms of linked reciprocal variables α and the terms $(N_x)_{cr}$, $(N_y)_{cr}$, and $(N_{xy})_{cr}$ are assumed to be constants evaluated by using the current set of detailed component level design variables. Interaction formula [Eq. (15)] buckling constraints are also used at the component level, where the terms $(N_x)_{cr}$, $(N_y)_{cr}$, and $(N_{xy})_{cr}$ are functions of the detailed panel design variables and the component loads N_x, N_y, and N_{xy} are obtained from the strains ϵ_x, ϵ_y, and γ_{xy}, which are generated by finite element analysis of the current system level design. These panel strains are assumed to be invariant during component synthesis.

In addition to panel buckling constraints, displacement, strength, and side constraints are also imposed at the system level. The strength requirements are introduced using upper and lower stress limits for TRUSS elements, Von Mises yield criteria for SSP elements, and Tsai-Azzi stress criteria for OLSR elements (equivalent thicknesses). The constraint deletion procedures of ACCESS 1 are used so that only critical and potentially critical constraints are retained. For the retained constraints explicit approximations are generated using first-order Taylor series expansions in terms of linked reciprocal variables. The total structural weight is minimized at the system level by executing one or more unconstrained minimizations, within the context of the interior penalty function algorithm.

The system level problem for fiber-composite hat-stiffened panel components is basically the same as in the fiber-composite sandwich-panel case. The basic difference is that some of the orthotropic stiffness properties of certain OLSR elements are set to zero in constructing the equivalent-thickness representation of the hat-stiffened panels. It should be recalled that the equivalent-thickness representation of sandwich panels requires four OLSR elements (see Fig. 2) while modeling the hat-stiffened panels requires five OLSR elements (see Fig. 4). Each of the OLSR finite elements, representing the equivalent thicknesses of a fiber-composite hat-stiffened panel component, have different material properties appropriate to their stiffness characteristics. In particular, note that the 0° material can only carry axial loading and the ±45° material in the stiffener can only carry axial loading and inplane shear. To model these characteristics the OLSR elements representing 0° material are taken to have axial stiffness as the only nonzero stiffness property and the OLSR elements representing +45° and −45° material in the stiffeners have zero stiffness in the direction transverse to the stiffeners. In both the sandwich and the hat-stiffened panels the thicknesses of +45° and −45° material are linked preserving the orthotropy of the panels. Therefore the number of independent system level design variables representing the panels is equal to three for both the sandwich and the hat-stiffened configurations.

The system level problem can be stated in mathematical form as follows:

Find $\boldsymbol{A}$, $\boldsymbol{t}$, $\boldsymbol{\tau}$ such that

$$W = \sum_{i \in I_T} \rho_i \ell_i A_i + \sum_{i \in I_0} \rho_i S_i t_i + \sum_{i \in I_S} \rho_i s_i \tau_i \rightarrow \min \tag{16}$$

and the following constraints are satisfied:

Side:

$$A_i^U \geq A_i \geq A_i^L \qquad i \epsilon I_T \tag{17}$$

$$t_i^U \geq t_i \geq t_i^L \qquad i \epsilon I_0 \tag{18}$$

$$\tau_i^U \geq \tau_i \geq \tau_i^L \qquad i \epsilon I_S \tag{19}$$

Nodal displacements:

$$u_i^U \geq u_{ik} \geq u_i^L \qquad i \epsilon I_u, \quad k=1,2,\ldots,K \tag{20}$$

Stress limits:

TRUSS:

$$\sigma_i^U \geq \sigma_{ik} \geq \sigma_i^L \qquad i \epsilon I_T, \quad k=1,2,\ldots,K \tag{21}$$

OLSR:

$$1-\left[\left(\frac{\sigma_{Lipk}}{F_{Li}}\right)^2-\left(\frac{\sigma_{Lipk}\sigma_{Tipk}}{F_{Li}^2}\right)+\left(\frac{\sigma_{Tipk}}{F_{Ti}}\right)^2+\left(\frac{\sigma_{LTipk}}{F_{LTi}}\right)^2\right] \geq 0$$

$$i \epsilon I_0, \quad p=1,2,\ldots,5 \quad k=1,2,\ldots,K \tag{22}$$

SSP:

$$\sigma_{ai} \geq \sigma_{eik} \qquad i \epsilon I_S, \quad k=1,2,\ldots,K \tag{23}$$

Gross panel buckling:

$$1-\left[\frac{N_{xjk}}{(N_{xjk})_{cr}^*}+\frac{N_{yjk}}{(N_{yjk})_{cr}^*}+\left(\frac{N_{xyjk}}{(N_{xyjk})_{cr}^*}\right)^2\right] \geq 0$$

$$j \epsilon M, \quad k=1,2,\ldots,K \tag{24}$$

The indices I_T, I_0, and I_S denote the total number of TRUSS, OLSR, and SSP elements, respectively. The density of the material is given by ρ in Eq. (16). The length of the truss member is given by ℓ_i while the surface area of OLSR and SSP elements are respectively given by S_i and s_i. The superscripts U and L denote the upper and lower limits for the associated quantities, K represents the total number of load conditions, I_u represents the number of constrained nodal displacements and u_{ik} denotes a nodal displacement component. Equation (22) represents the Tsai-Azzi stress criterion wherein the symbols σ_{Lipk} and σ_{Tipk} denote longitudinal and transverse stresses, respectively, and σ_{LTipk} represents shear stress. The subscripts L and T refer to the longitudinal and transverse axes of material orthotropy. The allowable stresses, F_{Li}, F_{Ti}, and F_{LTi} in Eq. (22) are given by

$$\begin{aligned} F_{Li} &= \sigma_{Li}^t \quad \text{if } \sigma_{Lipk} \geq 0 \\ &= \sigma_{Li}^c \quad \text{if } \sigma_{Lipk} < 0 \end{aligned} \tag{25}$$

$$\begin{aligned} F_{Ti} &= \sigma_{Ti}^t \quad \text{if } \sigma_{Tipk} \geq 0 \\ &= \sigma_{Ti}^c \quad \text{if } \sigma_{Tipk} < 0 \end{aligned} \tag{26}$$

$$F_{LTi} = \sigma_{LTi}^q \tag{27}$$

where σ_{Li}^t and σ_{Li}^c and longitudinal allowable stresses in tension and compression, respectively, σ_{Ti}^t and σ_{Ti}^c are transverse allowable stresses in tension and compression, respectively, and σ_{LTi}^q is the allowable shear stress. The integer p in Eq. (22) denotes a location in the stress field of the OLSR element. Since the normal stresses in each orthotropic linear stress rectangular (OLSR) element vary linearly, five points (the four corners and the centroid of each OLSR element) are checked using the Tsai-Azzi stress criteria. Equation (23) represents a constraint which prevents the Von Mises equivalent stress (σ_{eik}) from exceeding the allowable stress limit (σ_{ai}) for SSP elements. In Eq. (24) the in-plane resultant forces N_{xjk}, N_{yjk}, and N_{xyjk} are the summations of the equivalent uniform in-plane forces acting on the merged stack of OLSR elements. They (N_{xjk}, N_{yjk}, and N_{xyjk}) represent the loading on the jth panel component under the kth load condition. In Eq. (24) M denotes the number of panels. The critical in-plane loads $(N_{xjk})_{cr}^*$, $(N_{yjk})_{cr}^*$, and $(N_{xyjk})_{cr}^*$ used in Eq. (24) are computed based on detailed design variables at the end of the previous component level design modification stage, using Eqs. C9-C11 of Ref. 14. These critical loads are held invariant during each system level design modification stage.

Component Level

The in-plane force resultants N_x, N_y, and N_{xy} acting on the fiber composite panel are obtained from in-plane strains ϵ_x, ϵ_y, and γ_{xy}, using the familiar relationship

$$\{N\} = [A]\{\epsilon\} \tag{28}$$

which involves four independent membrane stiffness properties, namely, A_{11}, $A_{12}=A_{21}$, A_{22}, and A_{66}. These stiffness parameters when expressed explicitly in terms of the system design variables (equivalent thicknesses) are denoted by K_{rj} and when expressed explicitly in terms of component design variables they are denoted by H_{rj} ($r=1,2,3,4$). The in-plane stiffness properties H_{rj} in terms of the detailed design variables for the jth fiber-composite panel are given by

$$\begin{aligned} H_{1j} &= A_{11}(d_j) \qquad H_{2j} = A_{12}(d_j) \\ H_{3j} &= A_{22}(d_j) \qquad H_{4j} = A_{66}(d_j) \end{aligned} \tag{29}$$

where for sandwich panels

$$A_{mn}(d_j) = \sum_{i=1}^{3} (C'_{mn})_i t_i \qquad m,n=1,2,6 \tag{30}$$

and the $(C'_{mn})_i$ are constants depending upon the face sheet ply orientation angle θ_i and the elastic constants of the fiber-composite material (see Eqs. A3 of Ref. 14). In the case of hat-stiffened panels the $A_{mn}(d_j)$ are given by

$$A_{11}(d_j) = (C'_{11})_{\pm 45^\circ}\left(1+\frac{(2b_4+2b_2+b_3)}{(b_1+2b_4)}\right)t_2 + (C'_{11})_{0^\circ}\left(\frac{2b_3}{(b_1+2b_4)}\right)t_3 + (C'_{11})_{0^\circ}\left(\frac{2b_4}{(b_1+2b_4)}\right)t_4 \tag{31}$$

$$A_{12}(d_j) = (C'_{12})_{\pm 45^\circ} t_2 \tag{32}$$

$$A_{22}(d_j) = (C'_{22})_{\pm 45^\circ} t_2 \tag{33}$$

$$A_{66}(d_j) = (C'_{66})_{\pm 45^\circ}\left(1+\frac{(2b_4+2b_2+b_3)}{(b_1+2b_4)}\right)t_2 \tag{34}$$

Note that in Eqs. (30-34) the panel index j is omitted on the right-hand side of convenience.

Now denoting the stiffness of the component at the end of the foregoing system level design modification stage to be K_{rj}^*, the component level objective function becomes [see Eq. (8)]

$$m_j = \sum_{r=1}^{4} (K_{rj}^* - H_{rj})^2 \tag{35}$$

Replacing K^*_{rj} by A^*_{mn} and H_{rj} by $A_{mn}(d_j)$ in Eq. (35) yields

$$m_j(d_j) = [A^*_{11} - A_{11}(d_j)]^2 + [A^*_{12} - A_{12}(d_j)]^2 + [A^*_{22} - A_{22}(d_j)]^2 + [A^*_{66} - A_{66}(d_j)]^2 \quad (36)$$

where the A^*_{mn} are constant membrane stiffnesses based on the current system level equivalent thicknesses representing the panel.

The component level constraints include panel buckling, local buckling, and various side constraints. In the case of sandwich panels two distinct panel buckling analyses are available at the component level to predict buckling behavior of the panel: 1) a semiempirical buckling analysis based on the interaction formula given by Eq. (15), and 2) a more refined eigenvalue buckling analysis based on treating the sandwich panel as an equivalent orthotropic plate subject to uniform shear (N_{xy}) and linearly varying biaxial in-plane loading [$N_x(y)$ and $N_y(x)$] (see Ref. 14). The eigenvalue analysis is only used to check the feasibility of the final design. For hat-stiffened fiber-composite panels a simplified buckling analysis based on the method set forth in Ref. 12 is employed.

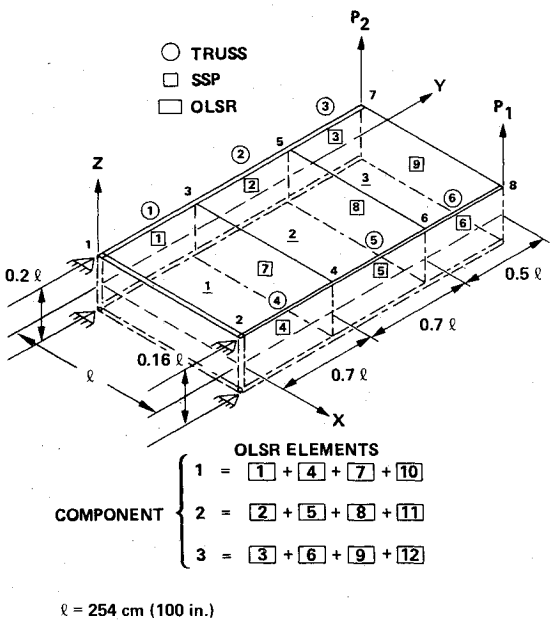

Fig. 5 Rectangular wing box with fiber-composite sandwich panels.

This buckling analysis was modified to take account of biaxial in-plane loading acting on the panel in conjunction with in-plane shear loading (see Ref. 14). This simplified treatment was developed using classical linear buckling analysis. Panel buckling is based on smeared stiffnesses and the well-known interaction formula. Local buckling constraints are based on the uncoupling assumption of simply supported boundary conditions along the lines where adjacent plate elements intersect. The accuracy of this simplified buckling analysis was favorably assessed in Ref. 13, using more rigorous methods based on linked plate eigenvalue type buckling analysis.

For wing box structures with fiber-composite hat-stiffened panels, the component level problem for the jth design component group can be stated as follows:

Find $t_2, t_3, t_4, b_1, b_2, b_3, b_4$ such that

$$m_j(d_j) = (A^*_{11} - A_{11})^2 + (A^*_{12} - A_{12})^2 + (A^*_{22} - A_{22})^2 + (A^*_{66} - A_{66})^2 \rightarrow \min \quad (37)$$

where A_{11}, A_{12}, A_{22}, and A_{66} are given by Eqs. (31-34) and the following constraints are satisfied.

Side:

$$t_i^U \geq t_i \geq t_i^L \qquad i=2,3,4 \quad (38)$$

$$b_i^U \geq b_i \geq b_i^L \qquad i=1,2,3,4 \quad (39)$$

$$b_1 \geq b_3 \quad (40)$$

$$b_1 \leq 2b_2 + b_3 \quad (41)$$

Gross panel buckling:

$$1 - \left[\frac{N^*_{xik}}{(N_{xik})_{cr}} + \frac{N^*_{yik}}{(N_{yik})_{cr}} + \left(\frac{N^*_{xyik}}{(N_{xyik})_{cr}} \right)^2 \right] \geq 0$$

$$i \epsilon I_j, \quad k = 1,2,\ldots,K \quad (42)$$

Local buckling:

Backup sheet (elements 1 and 4)

$$1 - \left[\frac{\tilde{N}_{xik\ell}}{(\tilde{N}_{xik\ell})_{cr}} + \frac{\tilde{N}_{yik\ell}}{(\tilde{N}_{yik\ell})_{cr}} + \left(\frac{\tilde{N}_{xyik\ell}}{(\tilde{N}_{xyik\ell})_{cr}} \right)^2 \right] \geq 0$$

$$i \epsilon I_j, \quad k = 1,2,\ldots,K \quad \ell = 1,4 \quad (43)$$

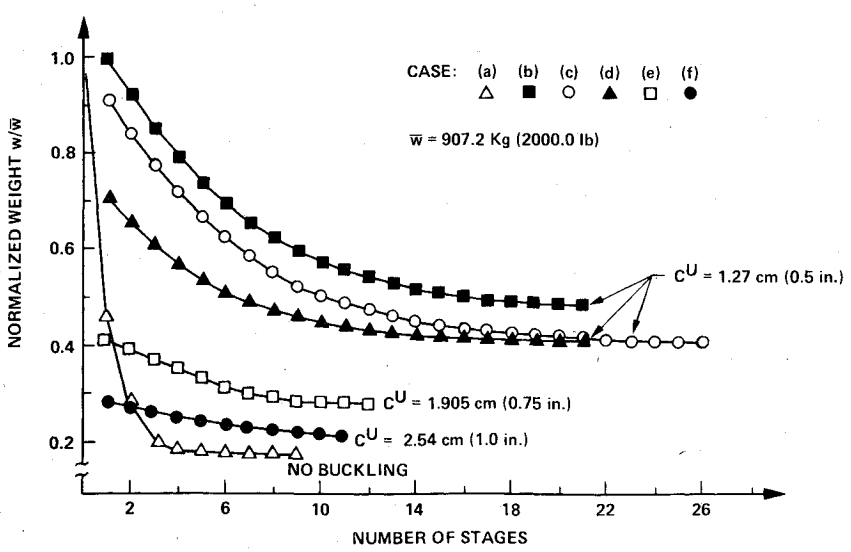

Fig. 6 Iteration histories for rectangular wing box with fiber-composite sandwich panels.

Table 1 Final design for fiber-composite sandwich components: rectangular wing box

	Component design variables	Without buckling constraints	With buckling constraints				
			Fixed TRUSS and SSP, cm (in.)				
		Case a	Case b[a]	Case c[a]	Case d[a]	Case e[b]	Case f[c]
1	$t(0°)$	0.3157	0.3959	0.0945	0.0605	0.2891	0.3274
		(0.1243)	(0.1599)	(0.0372)	(0.0238)	(0.1138)	(0.1289)
	$t(+45°)$	0.0254	0.3099	0.4707	0.4920	0.1852	0.0518
		(0.0100)	(0.1220)	(0.1853)	(0.1937)	(0.0729)	(0.0204)
	$t(-45°)$	0.0254	0.3099	0.4707	0.4920	0.1852	0.0518
		(0.0100)	(0.1220)	(0.1853)	(0.1937)	(0.0729)	(0.0204)
	$t(90°)$	0.0254	0.0729	0.1039	0.1034	0.0607	0.0323
		(0.0100)	(0.0287)	(0.0409)	(0.0407)	(0.0239)	(0.0127)
	C	...	1.27	1.27	1.27	1.905	2.54
			(0.50)	(0.50)	(0.50)	(0.75)	(1.00)
2	$t(0°)$	0.1478	0.2281	0.0805	0.0688	0.9776	0.1199
		(0.0582)	(0.0898)	(0.0317)	(0.0271)	(0.3849)	(0.0472)
	$t(+45°)$	0.0299	0.1755	0.2515	0.2527	0.1206	0.0554
		(0.0118)	(0.0691)	(0.0990)	(0.0995)	(0.0475)	(0.0218)
	$t(-45°)$	0.0299	0.1755	0.2515	0.2527	0.1206	0.0554
		(0.0118)	(0.0691)	(0.0990)	(0.0995)	(0.0475)	(0.0218)
	$t(90°)$	0.0254	0.1313	0.1829	0.1963	0.1387	0.0851
		(0.0100)	(0.0517)	(0.0720)	(0.0773)	(0.0546)	(0.0335)
	C	...	1.27	1.27	1.27	1.905	2.4767
			(0.50)	(0.50)	(0.50)	(0.75)	(0.9751)
3	$t(0°)$	0.0269	0.0841	0.0792	0.0704	0.0599	0.0599
		(0.0106)	(0.0331)	(0.0312)	(0.0277)	(0.0236)	(0.0236)
	$t(+45°)$	0.0366	0.0881	0.1092	0.1156	0.0747	0.0472
		(0.0144)	(0.0347)	(0.0430)	(0.0455)	(0.0294)	(0.0186)
	$t(-45°)$	0.0366	0.0881	0.1092	0.1156	0.0747	0.0472
		(0.0144)	(0.0347)	(0.0430)	(0.0455)	(0.0294)	(0.0186)
	$t(90°)$	0.0254	0.0965	0.1085	0.0922	0.0516	0.0478
		(0.0100)	(0.0380)	(0.0427)	(0.0363)	(0.0203)	(0.0188)
	C	...	1.0043	1.0376	1.0457	1.4381	1.7775
			(0.3954)	(0.4085)	(0.4117)	(0.5662)	(0.6998)
Panel weight, kg (lb)		100.10	287.67	310.93	311.34	197.30	132.72
		(220.68)	(634.20)	(685.48)	(686.38)	(434.96)	(292.60)
Structure weight, kg (lb)		164.79	440.73	375.85	376.34	261.99	197.42
		(363.30)	(971.62)	(828.60)	(829.68)	(577.58)	(435.22)
Stage		9	21	26	21	12	11

[a] $C^u = 1.27$ cm (0.5 in.). [b] $C^u = 1.905$ cm (0.75 in.). [c] $C^u = 2.54$ cm (1.0 in.).

Stiffener (elements 2 and 3)

$$1 - \left[\frac{\tilde{N}_{xik\ell}}{(\tilde{N}_{xik\ell})_{cr}} + \left(\frac{\tilde{N}_{xyik\ell}}{(\tilde{N}_{xyik\ell})_{cr}} \right)^2 \right] \geq 0$$

$$i \epsilon I_j, \qquad k = 1,2,\ldots,K \qquad \ell = 2,3 \tag{44}$$

The gross panel buckling constraints [Eq. (42)] involve invariant applied loads, while the critical buckling loads $[(N_{xik})_{cr}, (N_{yik})_{cr}, (N_{xyik})_{cr}]$ are nonlinear explicit functions of the component design variables d_j (see Eqs. C9-C11 of Ref. 14). In Eqs. (43) and (44) $\tilde{N}_{xik\ell}$, $\tilde{N}_{yik\ell}$, and $\tilde{N}_{xyik\ell}$ denote the element in-plane forces acting on element ℓ of the ith component, under load condition k. The expressions for these element loads are given by Eqs. D8-D10 of Ref. 14. In Eq. (43) the critical buckling loads $(\tilde{N}_{xik\ell})_{cr}$ and $(\tilde{N}_{yik\ell})_{cr}$ are calculated using Eq. C9 of Ref. 14, where a finite number of biaxial mode shapes are considered, and $(\tilde{N}_{xyik\ell})_{cr}$ is computed using a simple classical formula given in Eq. D1 of Ref. 14. Also in Eqs. (44), $(N_{xyik\ell})_{cr}$ and $(N_{xik\ell})_{cr}$ are computed using Eqs. D4 and D1 of Ref. 14, respectively. In Eqs. (42-44) the integer I_j represents the number of components that belong to the jth component design group while the index i represents the ith component in this design group. Since it is assumed that the strains are invariant during the component detailed design and because strength constraints are satisfied at the system level, they are omitted at the component level.

V. Numerical Results

The feasibility of extending multilevel methods to fiber composite panels is established by initially applying the method to the minimum weight design of wing box structures with fiber-composite sandwich panels. Minimum weight design results for a simple rectangular wing box structure subject to strength, displacement, panel buckling, and side constraints are obtained. Subsequently, the multilevel approach is applied to a minimum weight design of a delta wing with fiber-composite hat-stiffened panels. Additional numerical results can be found in Ref. 14.

Example 1: Wing Box with Sandwich Panels

Minimum weight designs for the idealized wing box structure shown in Fig. 5 are sought subject to various behavior and side constraints. This structure is assumed to be midplane symmetric, therefore only the upper half of the structure is considered in the design. The coverplate which is made up of three fiber-composite sandwich-panel components is idealized at the system level using 12 OLSR elements where each fiber-composite sandwich panel is modeled by stacking

four OLSR elements. The spars and ribs are modeled using six TRUSS elements and nine SSP elements. All of the TRUSS and SSP elements are assumed to have the same isotropic material properties (aluminum) and all the layers of OLSR elements are assumed to have the same composite material properties (high strength graphite-epoxy). Two distinct loading conditions are considered for this example: 1) $P_1 = 3.40$ kN (7500 lbf), $P_2 = 0$ kN; 2) $P_1 = 0$ kN, $P_2 = 6.80$ kN (15,000 lbf) (see Fig. 5). Displacement limitations of ± 7.62 cm (± 3 in.) in the Z direction are imposed on the free nodes.

For this simple rectangular wing box structure minimum weight designs were obtained for six different cases. Detailed design variable results for the panels are given in Table 1 and iteration histories are plotted in Fig. 6. In case a buckling constraints are ignored and in the other five cases (b-f) buckling constraints for each individual panel component are included. In case b the inclusion of the local buckling constraints increased the weight of the panels by 188% and the weight of the bars and shear panels by 138%. This unusual increase in the weight of the bars and the shear panels is attributed to the fact that the system level synthesis deals with the panel buckling constraints by transferring some of the panel forces to the bars and the shear panels. In cases c and d the bar cross sections and the shear panel thicknesses were frozen at the final design values obtained in case a. Although different panel design starting points were used for cases c and d, similar final designs, having almost identical weight are obtained (see Table 1). Fixing the bar cross sections and the shear panel thicknesses forces the panel to deal with its own buckling problem, rather than transferring load to the bars and shear panels. As expected, this leads to an increase in the $\pm 45°$ material thicknesses relative to case b. The weight of the panels (compared to case b) is increased by 8%, but the total structural weight is decreased by almost 15%. This difference in weight between cases b, c, and d indicates the existence of relative minima pockets in the design space. In cases b, c, and d panel buckling constraints for the two components nearest the root (1 and 2, see Fig. 5) are critical and the core depth for these two sandwich-panel components reaches the maximum allowable value of 1.27 cm (0.5 in.).

In addition to the foregoing results, the influence of available depth (for the sandwich-panel core) on the minimum weight design of the same idealized wing box structure has been examined (see Fig. 5). When larger available depth values are prescribed the buckling constraints are dealt with by increasing the core depth rather than by increasing the $\pm 45°$ material thicknesses (see Table 1). Increasing the maximum allowable core depth decreases the total structural weight drastically. For example, increasing the maximum core depth from 1.27 cm (0.5 in.) in case d to 2.54 cm (1.0 in.) in case f decreases the total structural weight by approximately 50%. Increasing the available core depth tends to alleviate the influence of panel buckling on the optimum design and the final design of case f is seen to have a material distribution which is approaching that found in case a where buckling constraints were ignored.

Example 2: Delta Wing with Hat-Stiffened Panels

The multilevel approach is applied to the minimum weight design of a previously studied[9] fiber-composite delta wing. The idealized wing is assumed to be symmetric with respect to its middle surface. Therefore only the upper half of the structure is considered in the design. The delta wing is modeled as shown in Fig. 7, where it is assumed that the cover plate consists of 28 fiber-composite hat-stiffened panels. These skin panels are modeled using 140 (5×28) OLSR elements. At the system level each fiber-composite panel is represented by a merged stack of five OLSR elements. It is to be understood that the material orientation angles are given with respect to the x reference coordinate in Fig. 7; for example, material oriented at 0° contains spanwise fibers. The vertical webs are modeled by 63 SSP elements. It is assumed

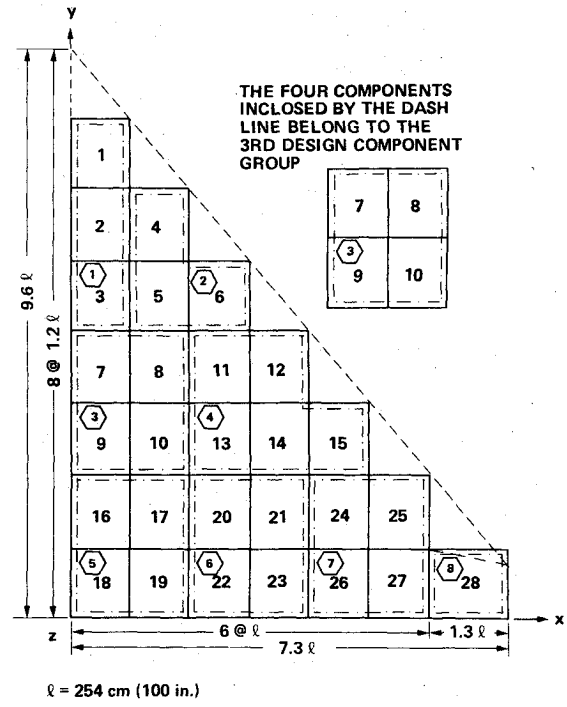

Fig. 7 Linked design components for delta wing.

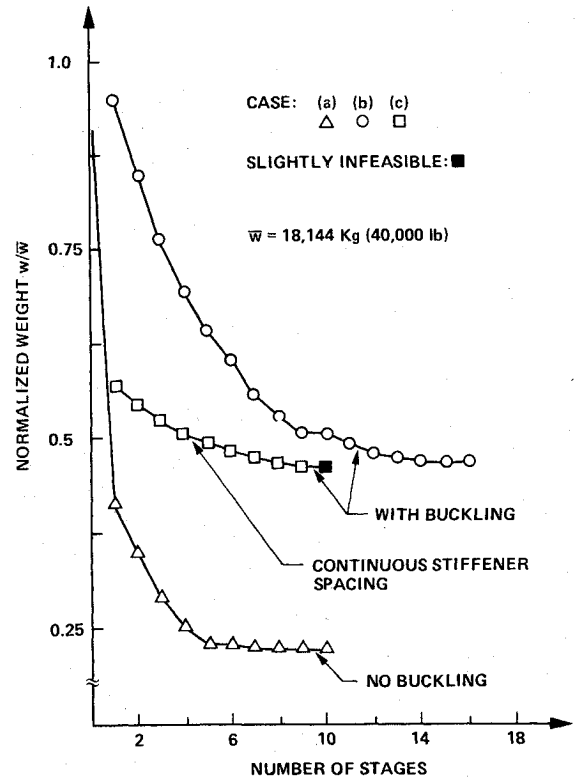

Fig. 8 Iteration histories for delta wing.

that the material properties for the lamina making up the skin are those of high-strength graphite-epoxy. The web material properties correspond to a representative titanium alloy. The wing is subjected to a single static load condition that is roughly equivalent to a uniformly distributed loading of 6.89 kN/m^2 (144 lb/ft^2). It should be noted that the allowable transverse stress is lower in tension than in compression for the fiber-composite materials. In general, if only the upper half of the symmetric wing is to be designed, the negative of the applied load should be considered as a second independent load condition, in order to insure a feasible design for the

Table 2 Final detailed design for delta wing, case c

Component design group no.	$t_2(\pm 45°)$ cm (in.)	$t_3(0°)$ cm (in.)	$t_4(0°)$ cm (in.)	b_1 cm (in.)	b_2 cm (in.)	b_3 cm (in.)	b_4 cm (in.)	Depth cm (in.)	Weight/ unit area, kg/m^2 (lb/in.^{2})
1	0.077051	0.181158	0.070518	2.7485	7.5745	2.7485	4.9967	7.5745	5.8848
	(0.030335)	(0.071322)	(0.027763)	(1.0821)	(2.9821)	(1.0821)	(1.9672)	(2.9821)	(0.00837)
2	0.085399	0.120200	0.041732	"	"	"	"	"	5.5403
	(0.033622)	(0.047323)	(0.016430)						(0.00788)
3	0.117028	0.286161	0.423316	3.1585	9.4496	2.6479	1.6624	9.44610	15.7884
	(0.046074)	(0.112662)	(0.16666)	(1.2435)	(3.7203)	(1.0425)	(0.6545)	(3.71894)	(0.022456)
4	0.127089	0.26668	0.152910	"	"	"	"	"	14.1460
	(0.050035)	(0.104992)	(0.060201)						(0.02012)
5	0.235267	1.098931	0.481813	3.2466	9.8374	3.2466	1.4760	9.8374	40.3357
	(0.092625)	(0.43265)	(0.18969)	(1.2782)	(3.8730)	(1.2782)	(0.5811)	(3.8730)	(0.05737)
6	0.152827	0.673913	0.343078	"	"	"	"	"	25.7749
	(0.060168)	(0.26532)	(0.13507)						(0.03666)
7	0.131630	0.271374	0.105138	"	"	"	"	"	15.7701
	(0.051823)	(0.10684)	(0.041393)						(0.02243)
8	0.141872	0.174061	0.150203	"	"	"	"	"	15.3201
	(0.055855)	(0.068528)	(0.059135)						(0.02179)

Table 3 Contribution of chordwise loading to the interaction formula for delta wing, case c

Component design group no.	Most critical panel	N_y/N_x	Percentage contribution to the interaction formula $N_x/(N_x)_{cr}$	$N_y/(N_y)_{cr}$	$[N_{xy}/(N_{xy})_{cr}]^2$
1	3	0.112	64.0	35.8	0.2
2	5	0.115	58.0	41.7	0.3
3	9	0.051	75.8	24.1	0.1
4	13	0.080	66.3	33.2	0.5
5	16	0.033	82.9	16.9	0.2
6	20	0.042	78.8	20.9	0.3
7	24	0.109	58.8	40.2	1.0
8	28	0.027	96.5	3.1	0.4

symmetric wing. However, the results reported here for the delta wing were obtained considering a single vertical load condition +6.89 kN/m^2 (+144 lb/ft^2) modeling only the upper half of the symmetric wing. Subsequently it was verified by analysis that the final designs reported are also feasible under the negative [6.89 kN/m^2 (−144 lb/ft^2)] load condition.

Design variable linking is used at both component and system levels to reduce the number of distinct fiber-composite hat-stiffened panels to eight (see Fig. 7). For example, it is understood that the four fiber-composite hat-stiffened panels (7, 8, 9, 10) in region 3 of Fig. 7 are to be identical. Therefore at the system level there are $8 \times 3 = 24$ independent design variables associated with skin panel equivalent thicknesses. Similarly, design variable linking is used for the SSP elements, leading to 11 independent design variables for the shear panels. Therefore the total number of system design variables adds up to 35.

This problem was solved using three consecutive runs as follows. In the first run, buckling constraints (panel and local) were excluded. In the second run, buckling constraints were included with the shear panel thicknesses fixed at the final values obtained in the first run. Finally, in the third run, the component level detailed spacing variables (b_i, see Fig. 3) were fixed in order to insure continuity from root to tip. The fixed spacing quantities (b_i) for the third run were obtained by a simple procedure which generates a feasible starting point for the continuous stiffener case. Iteration histories for these three runs (denoted as cases a, b, and c) are given in Fig. 8. In case a a minimum weight of 4018 kg (8859 lb) was obtained in ten stages. The breakdown of the final design weight between skin panels and the webs is 3608 kg (7954 lb) for the skin panels and 411 kg (905 lb) for the webs. In case b the inclusion of buckling constraints (panel and local) resulted in a minimum design weight of 8489 kg (18,716 lb) at stage 15. In case c, fixing the stiffener spacing and using tighter move limits at the system level resulted in a minimum design weight of 8394 kg (18,505 lb) at stage 9. Table 2 gives the final detailed panel designs for case c as well as the corresponding weight per unit surface area for each of the eight regions shown in Fig. 7. The weight distribution is intuitively reasonable, being heaviest at the root and decreasing toward the tip and leading edge. The most critical constraints at the final design obtained from case c are gross panel buckling in panels 3 and 5.

The inclusion of buckling constraints in cases b and c caused an increase of almost 110% in final design weight, compared to case a where buckling constraints are ignored (see Fig. 8). This drastic weight increase can be attributed to the presence of significant in-plane chordwise loading for the delta wing under uniform pressure load. Since the fiber-composite hat-stiffened panel shown in Fig. 3 is considerably weaker in chordwise bending, a small amount of compressive loading N_Y can cause a large increase in the final weight of the panel. In Table 3 the ratio of chordwise in-plane load to spanwise in-plane load (N_y/N_x), along with the percent contribution of the terms $N_x/(N_x)_{cr}$, $N_y/(N_y)_{cr}$, and $[N_{xy}/(N_{xy})_{cr}]^2$ to the interaction formula [see Eq. (15)] for the most critical panel in each region, are summarized. It is apparent from the information given in Table 3 that the contribution of $N_y/(N_y)_{cr}$ to the interaction formula is rather high. Disregarding region 8 (wing tip), the percent contribution of $N_y/(N_y)_{cr}$ to the interaction formula runs from a minimum value of 16.9% for panel 16 of region 5 to a maximum value of 41.7% for panel 5 of region 2. It is interesting to note that the previously identified most critical panels, i.e., 3 and 5, also exhibit large $N_y/(N_y)_{cr}$ values in Table 3.

VI. Conclusions

The multilevel method has been successfully extended to wing box structures involving either sandwich panels with fiber-composite face sheets or hat-stiffened fiber-composite panels. The multilevel approach facilitates the inclusions of panel and local buckling constraints in addition to strength and displacement limitations. Assumed stress orthotropic elements and panel buckling constraints have been added into ACCESS 1 to create the system level portion of the design procedure. At the component level change of stiffness is taken as the objective function to be minimized, while the panel and local buckling analyses used parallel those reported in Ref. 12. A quadratic extended interior penalty function algorithm is used at both the component and system levels and its inherent constraint repulsion characteristic enhances convergence by reducing coupling between the system and component optimization problems. The multilevel method employed here may be interpreted as a heuristic decomposition technique in which the formulation is guided by physical insight regarding the uncoupling of structural behavior. The large number of design variables needed to describe the detail design of numerous stiffened fiber-composite panels and the importance of local buckling constraints underscores the need for a multilevel approach to optimum design of structural systems involving such components.

Acknowledgment

This research was supported by NASA Research Grant NSG 1490.

References

[1] Felton, L. P. and Hofmeister, L. D., "Optimized Components in Truss Synthesis," *AIAA Journal,* Vol. 6, Dec. 1968, pp. 2434-2436.

[2] Felton, L. P., Nelson, R. B., and Bronowicki, A. J., "Thin-Walled Elements in Truss Synthesis," *AIAA Journal,* Vol. 11, Dec. 1973, pp. 1780-1782.

[3] Felton, L. P. and Fuchs, M. B., "Simplified Direct Optimization of Tubular Truss Structures," *International Journal of Numerical Methods in Engineering,* Vol. 17, Apr. 1981, pp. 601-613.

[4] Giles, G. L., "Procedure for Automating Aircraft Wing Structural Design," *Journal of the Structural Division, ASCE,* Vol. 97, No. ST1, Jan. 1971, pp. 99-113.

[5] Sobieszczanski, J. and Leondorf, D., "A Mixed Optimization Method for Automated Design of the Fuselage Structures," *Journal of Aircraft,* Vol. 9, Dec. 1972, pp. 805-822.

[6] Schmit, L. A. and Ramanathan, R. K., "Multilevel Approach to Minimum Weight Design including Buckling Constraints," *AIAA Journal,* Vol. 16, Feb. 1978, pp. 97-104.

[7] Schmit, L. A. and Miura, H., "A New Structural Analysis/Synthesis Capability—ACCESS 1," *AIAA Journal,* Vol. 14, May 1976, pp. 661-671.

[8] Schmit, L. A. and Miura, H., "Approximation Concepts for Efficient Structural Synthesis," NASA CR 2552, March 1976.

[9] Schmit, L. A. and Miura, H., "An Advanced Structural Analysis/Synthesis Capability-ACCESS 2," *International Journal of Numerical Methods in Engineering,* Vol. 12, Feb. 1978, pp. 353-377.

[10] Haftka, R. T. and Starnes, J. H., "Applications of a Quadratic Extended Interior Penalty Function for Structural Optimization," *AIAA Journal,* Vol. 14, June 1976, pp. 718-724.

[11] Haftka, R. T., "Automated Procedure for Design of Wing Structures to Satisfy Strength and Flutter Requirements," NASA TN D-7264, July 1973.

[12] Stroud, W. J. and Agranoff, N., "Minimum Mass Design of Filamentary Composite Panaels under Combined Loads: Design Procedure Based on Simplified Buckling Equations," NASA TN D-8275, Oct. 1976.

[13] Stroud, W. J., Agranoff, N., and Anderson, M. S., "Minimum Mass Design of Filamentary Composite Panels under Combined Loads: Design Procedure based on Rigorous Buckling Analysis," NASA TN D-8417, July 1977.

[14] Mehrinfar, M., "Multilevel Optimum Design on Wing Box Structures with Fiber Composite Panel Components," Ph.D. Thesis, Mechanics and Structures Department, University of California, Los Angeles, Calif., 1980.